Effects of frustration on fluctuation-dissipation relations

Federico Corberi,[1,*] Manoj Kumar,[2,†] Eugenio Lippiello,[3,‡] and Sanjay Puri[4,§]

[1]*Dipartimento di Fisica "E. R. Caianiello", and INFN, Gruppo Collegato di Salerno, and CNISM, Unità di Salerno, Università di Salerno, via Giovanni Paolo II 132, 84084 Fisciano (SA), Italy*

[2]*International Centre for Theoretical Sciences, Tata Institute of Fundamental Research, Bengaluru 560089, India*

[3]*Department of Mathematics and Physics, University of Campania "L. Vanvitelli", Viale Lincoln 5, 81100 Caserta, Italy*

[4]*School of Physical Sciences, Jawaharlal Nehru University, New Delhi 110067, India*

(Received 25 September 2018; published 17 January 2019)

We study numerically the aging properties of the two-dimensional Ising model with quenched disorder considered in our recent paper [Phys. Rev. E **95**, 062136 (2017)], where frustration can be tuned by varying the fraction of antiferromagnetic interactions. Specifically, we focus on the scaling properties of the autocorrelation and linear response functions after a quench of the model to a low temperature. We find that the interplay between equilibrium and aging occurs differently in the various regions of the phase diagram of the model. When the quench is made into the ferromagnetic phase the two-time quantities are made by the sum of an equilibrium and an aging part, whereas in the paramagnetic phase these parts combine in a multiplicative way. Scaling forms are shown to be obeyed with good accuracy, and the corresponding exponents and scaling functions are determined and discussed in the framework of what is known in clean and disordered systems.

DOI: 10.1103/PhysRevE.99.012131

I. INTRODUCTION

After a quench from a high-temperature to a low-temperature phase, a system enters a dynamical state which is generally characterized by slow evolution and aging. In the simplest cases, as in binary systems without quenched disorder, the kinetics is quite well understood. Domains of the two low-temperature equilibrium phases form and evolve with an average size $L(t) \propto t^{1/z}$ growing algebraically as time elapses. A prominent feature is the existence of dynamical scaling, namely, the fact that configurations of the same system at different times happen to be self similar, namely, statistically equal except for a trivial rescaling of lengths by a factor $L(t)$. As a consequence, observable quantities such as correlation functions and linear response functions take a definite scaling form, similarly to what happens in static critical phenomena.

The value of the dynamical exponent z and of other exponents entering such scaling forms, together with the behavior of the scaling functions, are known to exhibit universal properties, being dependent only on few relevant features, e.g., the scalar or vectorial nature of the system, and the presence of conservation laws or hydrodynamic interactions. In addition, the connection between static and dynamic properties derived in Ref. [1] allows one to infer the form of the so-called fluctuation-dissipation plot, namely, the asymptotic relation between two two-time quantities, the autocorrelation function and the associated linear response function, starting from the well-known structure of the broken-symmetry equilibrium state.

Such a good comprehension of the universal properties of the kinetics is, however, lost as soon as quenched disorder is present in the system. This is true not only in the case when strong disorder and frustration are present, such as in the emblematic case of spin glasses, but even for tiny amounts of quenched randomness. Indeed, even in the cases when a weak disorder does not produce relevant changes in the static properties, the nonequilibrium kinetics is usually affected in a dramatic way. In magnets, for instance, the presence of unequal, though ferromagnetic, coupling constants may change the exponent of the power-law growth of $L(t)$ with respect to the clean case or even turn $L(t)$ into a logarithmic form [2]. Similar features are observed in the presence of other kinds of quenched randomness [3–6].

When disorder is stronger and associated with frustration the problem is by far much more complicated and the interpretation of both the static structure and the nonequilibrium properties are still debated issues [7]. In this scenario, understanding the properties of two-time quantities and of their relation might represent an important contribution to the understanding of both the static and the dynamics, given the bridge between these two aspects provided by the fluctuation-dissipation relation discussed above. However, given the very slow and complex evolution affecting these systems, arriving to a conclusive numerical evidence on the asymptotic form of correlation and response functions often represents a formidable task.

In this paper we tackle this matter from a different perspective. Instead of facing the hard problem straightforwardly, by measuring two-time quantities directly in the fully frustrated system, we try to narrow the difficulty, starting from the well-understood clean ferromagnetic case and moving toward the

*corberi@sa.infn.it
†manojkmr8788@gmail.com
‡eugenio.lippiello@unina2.it
§purijnu@gmail.com

fully frustrated case in a model where the amount of disorder and frustration can be tuned at will. We do that by computing numerically the spin autocorrelation function $C(t,t_w) = N^{-1}\sum_{i=1}^{N}\langle s_i(t)s_i(t_w)\rangle$ and the associated linear response in a random-bond Ising model with an adjustable fraction a of antiferromagnetic bonds. In this way, we can study the modifications of the properties of two-time quantities when, starting from the well-known clean ferromagnet with $a = 0$, one moves into a phase where frustration is relevant.

It is important to highlight the important features in our modeling and results presented in this paper. The first significant aspect we address is the universality of two-time quantities. According to the *superuniversality* hypothesis [8,9], once expressed in a scaling form in terms of the growing length $L(t)$, exponents and scaling functions of different quantities in a coarsening system are independent of the nature and magnitude of quenched disorder. We find that this is not the case in the present model. In particular, the *response function exponent*, which has been the subject of many recent studies [10–23], turns out to be strongly disorder-dependent. Our results show that it vanishes at the transition from the ferromagnetic to the paramagnetic phase.

Our model does not exhibit a spin-glass phase in the $d = 2$ case considered in this paper. Notwithstanding, spin-glass order is expected at zero temperature when frustration is strong enough. The $d = 2$ case has the advantage that low-temperature equilibrium states can be determined relatively rapidly, thus allowing us to consider systems with sufficiently large sizes. A precise determination and understanding of the two-time quantities is therefore possible, both in the equilibrium states and in the nonequilibrium evolution. This is the second important aspect of our present study. In this context, we use an out-of-equilibrium generalization of the fluctuation-dissipation theorem [21,24–27]. Thus, we are able to cleanly address the issue of how the equilibrium and the aging degrees of freedom combine to determine the scaling forms of correlation and response functions. This is an important prerequisite to understand the properties of the fluctuation-dissipation relation [21,24–27]. To the best of our knowledge, this approach has never been pursued for this kind of model. We find that the structure of the phase diagram (see Fig. 1) is faithfully reflected in the properties of the two-time quantities. The phase diagram shows a ferromagnetic phase for $a < a_f$ and an antiferromagnetic phase for $a > a_a$. These are separated by a paramagnetic region (with spin-glass order at $T = 0$) for $a_f \leqslant a \leqslant a_a$. The corresponding properties of the two-time quantities are as follows:

(a) In the ferromagnetic phase ($a < a_f$) (and similarly in the antiferromagnetic phase with $a > a_a$), the two-time quantities have an additive form. For example, the autocorrelation function obeys $C(t,t_w) = C_{\rm eq}(t - t_w) + C_{\rm ag}(t,t_w)$. Here, $C_{\rm eq}$ is the equilibrium correlation, and the aging part $C_{\rm ag}$ obeys a scaling form $C_{\rm ag}(t,t_w) = c[L(t)/L(t_w)]$ (c is a scaling function). (An analogous behavior is shown by the response function.) This structure is generic, but the scaling functions and the response function exponent depend on a, with the latter vanishing at $a = a_f$. The fluctuation-dissipation plot has the usual broken-line shape of ferromagnetic models [12].

(b) At the critical point $a = a_f$ (or, equivalently, $a = a_a$), the additive structure turns into a multiplicative one

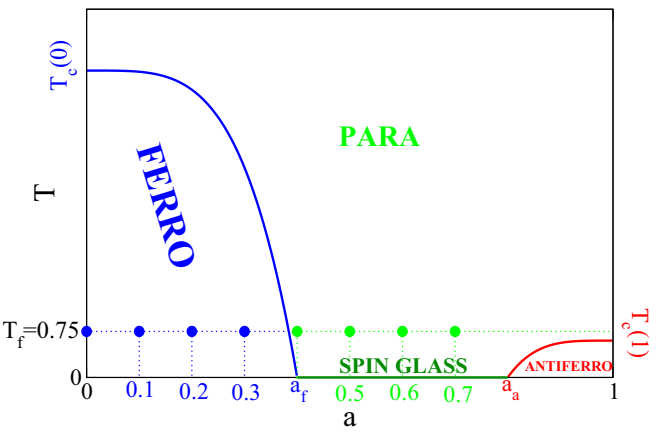

FIG. 1. Pictorial representation of the phase-diagram of the model. The heavy dots are the points where our simulations are carried out.

$C(t,t_w) = C_{\rm eq}(t - t_w)C_{\rm ag}(t,t_w)$, with the scaling properties of $C_{\rm ag}$ as discussed above. The fluctuation-dissipation plot also changes radically, and now approaches the equilibrium linear behavior expected in systems at criticality [28,29]. These properties are observed in the whole frustration-dominated paramagnetic region $a_f \leqslant a \leqslant a_a$.

This paper is organized as follows: In Sec. II we introduce and describe the model and the quantities that will be numerically computed. In Sec. III we briefly review what is known about the scaling properties of two-time quantities in clean and disordered systems. In Sec. IV we present and discuss the outcomes of our numerical simulations. Sec. V concludes the paper with a summary and a discussion of our findings and of possible future perspectives.

II. MODEL AND OBSERVABLE QUANTITIES

In this paper we consider the spin model governed by the Hamiltonian

$$\mathcal{H}(\{s_i\}) = -\sum_{\langle ij\rangle} J_{ij}s_is_j, \tag{1}$$

where $s_i = \pm 1$, $\langle ij\rangle$ denotes nearest neighbors sites of a lattice, and $J_{ij} = J_0 + \xi_{ij}$ are uncorrelated stochastic random couplings with $J_0 > 0$ and ξ_{ij} extracted from a bimodal distribution

$$P(\xi) = a\,\delta_{\xi,-K} + (1-a)\,\delta_{\xi,K}, \tag{2}$$

where $K > J_0$, $0 \leqslant a \leqslant 1$ is the fraction of antiferromagnetic bonds, and δ is a Kronecker function. We will consider a square lattice with N spins, periodic boundary conditions, $J_0 = 1$ and $K = 5/4$ in the following. We also set the Boltzmann constant $k_B = 1$. With these parameters the model has been previously characterized in Ref. [30]. A similar model was introduced and studied in Refs. [31,32].

It was shown [30] that the model has a ferromagnetic phase for sufficiently low temperatures $T < T_c(a)$, where $T_c(a)$ is a critical temperature vanishing in the limit $a \to a_f^-$, with $a_f \simeq 0.4$, as pictorially sketched in Fig. 1 (the reason for using such a rough representation is that the real phase-diagram of this model, namely, a determination of T_c for all values

of a, is not currently available). For large values of a an antiferromagnetic phase exists (which will not be considered in this paper) for $T < T_c(a)$ (we use the same symbol as for the ferromagnetic case for simplicity), where $T_c(a) \to 0$ as $a \to a_a^+$. For intermediate values of a the equilibrium state of the system is paramagnetic and disordered except, possibly, right at $T = 0$ where for $a_f \leqslant a \leqslant a_a$ a spin-glass phase is expected.

In the following we will consider the nonequilibrium kinetics obtained by quenching the present model from an equilibrium state at infinite temperature to a sufficiently low final temperature T_f. The values of a studied in our simulation, and the value of T_f considered, are also shown in Fig. 1.

To detect the build-up of spatial correlations an average size of ordered regions at time t can be defined as

$$L(t) = [E(t) - E_{\rm eq}]^{-1}, \tag{3}$$

where $E(t)$ is the energy per spin of the system at the current time t and $E_{\rm eq}$ is the same quantity computed at equilibrium at the temperature $T = T_f$. This definition of an ordering length is standard in ferromagnetic systems. A thorough discussion, together with a determination of this quantity, can be found in Ref. [30].

In this paper we focus on the scaling properties of the two-time quantities that we detail below. The autocorrelation function is defined as

$$C(t, t_w) = \frac{1}{N} \sum_{i=1}^{N} [\langle s_i(t) s_i(t_w) \rangle - \langle s_i(t) \rangle \langle s_i(t_w) \rangle], \tag{4}$$

with $t \geqslant t_w$. Here $\langle \dots \rangle$ means both the thermal average, namely, over initial conditions and dynamical trajectories, and over the realizations of the quenched disorder. Notice that, after a quench from high temperature, symmetry is not broken at any finite time (in the thermodynamic limit) and hence the subtraction term on the right-hand side of Eq. (4) is immaterial (however, it will be relevant when we will introduce the autocorrelation in equilibrium $C_{\rm eq}$, below). The impulsive autoresponse function is defined as

$$R(t, t_w) = \frac{1}{N} \sum_{i=1}^{N} \left. \frac{\delta \langle s_i(t) \rangle_h}{\delta h_i(t_w)} \right|_{h=0}, \tag{5}$$

where $h_i(t)$ is a time-dependent magnetic field and $\langle \dots \rangle_h$ means an average in the presence of such field. Since this quantity is very noisy it is customary to measure the so called *integrated* autoresponse function, sometimes also denoted as the *zero-field cooled susceptibility*,

$$\chi(t, t_w) = \int_{t_w}^{t} dt' \, R(t, t'). \tag{6}$$

This quantity has an enhanced signal/noise ratio and is more suited to enlighten the scaling properties, as discussed in Ref. [16]. To compute χ numerically without applying the small perturbation we use the generalization of the fluctuation-dissipation theorem to nonequilibrium states derived in Refs. [21,24–27].

III. SCALING BEHAVIORS

A. Nondisordered systems

The scaling behavior of the two-time quantities introduced in Sec. II are quite well understood in ferromagnetic models without quenched disorder and short-range interactions [7,33]. In this case slow relaxation is observed when a system in equilibrium at $T > T_c$ is quenched either to the critical temperature T_c or to any final temperature $T_f < T_c$, including $T_f = 0$. In any case, after a transient, a dynamical state is entered where an ordering length grows algebraically in time as $L(t) \sim t^{1/z}$ [34], where $t = 0$ is the quench instant. Referring to the case of a purely relaxational dynamics with a nonconserved order parameter considered in the present paper the exponent z takes a value $z = 2$ independent of both T_f and spatial dimension d in all quenches with $T_f < T_c$. Instead, when the quench is made at $T_f = T_c$, z coincides with the dynamical critical exponent z_c, which depends on d and becomes $z_c = 2$ only at the lower critical dimension d_L [35].

It should be stressed that, although the unbounded growth of $L(t)$ makes the nonstationary character of the dynamics manifest, on sufficiently short time and space scales local equilibration takes place. For instance, in the ferromagnetic systems we are considering now, thermal fluctuations well inside the overall ordered growing domains, whose typical size is the equilibrium coherence length $\xi_{\rm eq}(T_f) \ll L(t)$, behave as in an equilibrium state at $T = T_f$. As we will see shortly, the aging (i.e., nonequilibrium) and equilibrium features may combine differently in determining the scaling properties of the observable quantities.

The self-similarity of configurations as time elapses determines a dynamical scaling symmetry which, in turn, informs observable quantities such as $C(t, t_w)$ and $R(t, t_w)$ or $\chi(t, t_w)$. As discussed in Ref. [33], the scaling properties of these functions depend, in turn, on the kind of quench. More precisely one has three different behaviors corresponding to (i) a subcritical quench to $T_f < T_c$, (ii) a critical quench to $T_f = T_c > 0$ for $d > d_L$, and (iii) a critical quench to $T_f = T_c = 0$ for $d = d_L$. We discuss them separately below.

1. Subcritical quench to $T_f < T_c$ ($d > d_L$)

In this case, for large t_w, C and R take the forms [12]

$$C(t, t_w) = C_{\rm eq}(t - t_w) + C_{\rm ag}(t, t_w), \tag{7}$$

$$R(t, t_w) = R_{\rm eq}(t - t_w) + R_{\rm ag}(t, t_w), \tag{8}$$

where $C_{\rm eq}$ and $C_{\rm ag}$ (and similarly for R) are an equilibrium and an aging term, respectively. The former is the one that one should have in a system in equilibrium at the final temperature of the quench and obeys the fluctuation-dissipation theorem,

$$T R_{\rm eq}(t - t_w) = -dC_{\rm eq}(t - t_w)/dt, \tag{9}$$

and the latter is what is left over. Notice that this is an additive structure where equilibrium and nonequilibrium contributions sum up. The aging parts obey a scaling form

$$C_{\rm ag}(t, t_w) = c\left[\frac{L(t)}{L(t_w)}\right] \tag{10}$$

and

$$R_{\rm ag}(t,t_w) = L(t_w)^{-(z+\alpha)} r\left[\frac{L(t)}{L(t_w)}\right], \tag{11}$$

where c and r are scaling functions and α is the response function exponent. Notice that Eq. (10) could also be written as $C_{\rm ag}(t,t_w) = L(t_w)^{-\beta} c[\frac{L(t)}{L(t_w)}]$ with $\beta = 0$ and this implies [36] that the domains grow with a dimension $d - z\beta/2 = d$, namely, they are compact for this kind of quench. The exponent $\alpha > 0$ is not related to the behavior of C (at variance with the case of a critical quench, see Sec. III A 2 below), and its determination has been the subject of many studies [10–23,38], both on the analytical and numerical side.

It is a trivial consequence of Eqs. (8) and (11) that an additive structure informs also the integrated response, $\chi(t,t_w) = \chi_{\rm eq}(t-t_w) + \chi_{\rm ag}(t,t_w)$, with

$$\chi_{\rm ag}(t,t_w) = L(t_w)^{-\alpha} f\left[\frac{L(t)}{L(t_w)}\right]. \tag{12}$$

From the properties discussed above we see that in the short time-difference regime one has

$$C(t,t_w) = C_{\rm eq}(t-t_w) + q_{\rm EA}, \tag{13}$$

where $q_{\rm EA} = c(1)$ is the so-called Edwards-Anderson order parameter, which, for a ferromagnet, amounts to the squared spontaneous magnetization at equilibrium at $T = T_f$. Instead, in the large time-difference regime, namely, with $t - t_w \to \infty$ with fixed $L(t)/L(t_w)$, one has

$$C(t,t_w) = C_{\rm ag}(t,t_w). \tag{14}$$

Starting from these behavior it is easy to show [33] that C has the weak ergodicity breaking property $\lim_{t-t_w\to\infty} \lim_{t_w\to\infty (t-t_w \text{ fixed})} C(t,t_w) \neq \lim_{t_w\to\infty} \lim_{t-t_w\to\infty (t_w \text{ fixed})} C(t,t_w)$, which is associated to the broken ergodicity of the equilibrium state below T_c. This is at variance to what happens in the critical quench (see Sec. III A 2), where spontaneous magnetization does not develop and ergodicity occurs.

For the response function one has that $R_{\rm eq}$ obeys the fluctuation-dissipation theorem Eq. (9) with respect to $C_{\rm eq}$ and vanishes in the large time-difference regime while, conversely, $R_{\rm ag}$ vanish in the short time-difference regime.

Let us mention that the above features are independent of T_f and hence apply down to $T_f = 0$, since temperature is an irrelevant parameter in the renormalization group sense [39,40].

2. Critical quench to $T_f = T_c > 0$ ($d > d_L$)

In this case Eqs. (7) and (8) change to [28,29]

$$C(t,t_w) = C_{\rm eq}(t-t_w) C_{\rm ag}(t,t_w), \tag{15}$$

$$R(t,t_w) = R_{\rm eq}(t-t_w) R_{\rm ag}(t,t_w), \tag{16}$$

where $C_{\rm ag}$ and $R_{\rm ag}$ are the nonequilibrium contributions which depend only on the ratio $L(t)/L(t_w)$

$$C_{\rm ag}(t,t_w) = c\left[\frac{L(t)}{L(t_w)}\right], \tag{17}$$

$$R_{\rm ag}(t,t_w) = r\left[\frac{L(t)}{L(t_w)}\right], \tag{18}$$

with $c(x)$ and $r(x)$ scaling functions [different from the ones of Eqs. (10) and (11)], whereas

$$C_{\rm eq}(t-t_w) = (t - t_w + t_0)^{-B} \tag{19}$$

and

$$R_{\rm eq}(t-t_w) = (t - t_w + t_0)^{-(1+A)}, \tag{20}$$

are the equilibrium autocorrelation and response functions at $T = T_c$. Here A and B are the autocorrelation and response exponents, t_0 is a microscopic time, and the fluctuation-dissipation theorem Eq. (9) implies $A = B$. A scaling relation links the actual value of these exponents to the usual equilibrium critical static and dynamic ones η and z through $A = B = (d - 2 + \eta)/z$ which, in turn, implies [36] a fractal dimension $D = d - zB/2$ of the critical correlated clusters. Notice that $B \to 0$ as $d \to d_L^+$, implying that critical clusters become compact objects in this limit.

Let us stress that the structure Eqs. (15) and (16) means that the equilibrium part and the nonequilibrium one of two-time quantities enter in a multiplicative manner. Replacing the form Eqs. (16) and (18) into Eq. (6) one finds that no particular scaling property shows up in $\chi(t,t_w)$. However, it can be shown [37] that the quantity $L(t_w)^{\gamma}[1 - T_f \chi(t,t_w)]$, which represents the distance from the equilibrium static value, scales as

$$L(t_w)^{\gamma}[1 - T_f \chi(t,t_w)] = L(t_w)^{-\gamma} g\left[\frac{L(t)}{L(t_w)}\right], \tag{21}$$

where $\gamma = zB$ and g is a scaling function.

According to Eqs. (15) and (16) in the short time difference regime, namely, letting t_w become large while keeping $t - t_w$ fixed, one gets

$$C(t,t_w) = C_{\rm eq}(t-t_w) C_{\rm ag}(1) \propto C_{\rm eq}(t-t_w), \tag{22}$$

$$R(t,t_w) = R_{\rm eq}(t-t_w) R_{\rm ag}(1) \propto R_{\rm eq}(t-t_w). \tag{23}$$

3. Quenches to $T_f = 0$ with $d = d_L$

At d_L it is $T_c = 0$ and hence $T_f = 0$ can be viewed also as a limiting case of a critical quench. However, since an equilibrium system without quenched disorder is perfectly ordered at $T = 0$, it is clear that the scaling structure of two-time quantities must be akin to the one of the subcritical quenches, namely, additive, because weak ergodicity breaking must occur. Moreover $C = C_{\rm ag}$, since the equilibrium state at $T = 0$ has no dynamics. The same property is shared by $\chi_{\rm eq}$, but only in scalar systems with a discrete (up-down) symmetry, while $\chi_{\rm eq}$ does not vanish in vectorial systems with continuous symmetry, due to the presence of Goldstone modes. The distinguishing feature of the quench at $T_f = 0$ with $d = d_L$ is that $\alpha = 0$ in this case [11,12,16,41–47].

B. Disordered systems

Let us now briefly discuss the modifications due the presence of quenched disorder (see also Refs. [48,49] for a discussion of this topic). Since the matter is, in some cases, still debated, we will make only reference to some systems where a good understanding and accepted analytic background is available.

It turns out that the presence of quenched disorder may introduce a different scaling pattern with respect to those encountered in so far. When systems such as p-spins [50] or mean-field spin glasses [51,52] are quenched to a phase with $q_{\rm EA} > 0$, namely, to below a finite critical temperature, one has an additive structure, as expected. However, at variance with the nondisordered case discussed in Sec. III A 1, one has a value $\alpha = 0$ of the response function exponent for $d > d_L$. We remind that $\alpha = 0$ is found also in clean ferromagnetic systems but only at d_L, where the quench can only be made at $T_f = 0$ and, due to that, $C_{\rm eq}$ and $\chi_{\rm eq}$ vanish identically in system with a scalar order parameter. Conversely, in the aforementioned disordered scalar models, for $d > d_L$ quenches with $T_f > 0$ display both $\alpha = 0$ and a nontrivial $C_{\rm eq}$ and $\chi_{\rm eq}$.

IV. NUMERICAL RESULTS

We have run a set of simulations both of a system quenched from infinite temperature to a final temperature $T_f = 0.75$ (we set the Boltzmann constant equal to unity) and, in parallel, of the same system in equilibrium at the final temperature of the quench. To equilibrate the system we first found the ground state by means of the algorithm discussed in Ref. [53], which allows us to determine the configuration in polynomial time. Then, using the ground state as an initial condition, we have equilibrated the system at the working temperature by means of standard Monte Carlo techniques. We have simulated two-dimensional systems on a square lattice with 512×512 spins. This size is free from finite-size effects in the accessed time window. For any run we have taken an average over 10^3 different realizations. Monte Carlo moves use Glauber transition rates.

The chosen value of T_f has been shown to be a reasonable compromise between the attempt to study the low-temperature behavior of the model and the need to avoid the sluggish dynamics observed when T_f is too low. Our simulations are performed for several values of a to span both the ferromagnetic and the paramagnetic region (the antiferromagnetic phase is expected to give similar results to the ferromagnetic one). A visual summary of the various quenches considered in this study is provided in Fig. 1. We also acknowledge that a study of the autocorrelation function in a related model (but restricted to the case $d = 3$, which is rather different due to the presence of a spin-glass phase at finite temperature) was carried out in Ref. [54]. To the best of our knowledge, the response function has never been considered.

The behavior of the ordering length $L(t)$ after a quench of the model has been thoroughly discussed in Ref. [30]. For completeness we show in Fig. 2 its behavior for the values of a that will be considered in this paper. Here and in the following, time is measured in units of Monte Carlo steps. Notice that in Fig. 2 we normalize $L(t)$ by its value at an early time ($t = 4$)

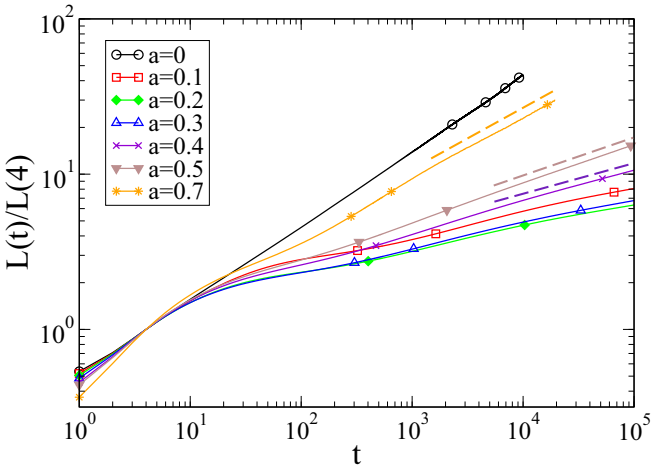

FIG. 2. $L(t)$ is plotted against time for different values of a (see legend) after a quench of the model to $T_f = 0.75$. The dashed lines slightly above the right part of some of the curves are the best algebraic fits. Specifically, the indigo line is the behavior $x^{1/5}$, the dashed brown is the one $x^{1/4}$, and the dashed orange is $x^{1/2.56}$.

to better compare curves with different a. One observes that, in the range of times considered, $L(t)$ keeps growing for any value of a. The growth is faster in the pure case [when one has $L(t) \propto t^{1/2}$] than for any other value of a, and the slowest case occurs with $a = 0.2$. The fact that $L(t)$ keeps growing also in the paramagnetic phase can be interpreted as due to the proximity of the spin-glass phase at $T = 0$, for $a_f < a < a_a$, as will be further discussed below.

In the following we will discuss the behavior of the two-time quantities introduced in Sec. II, separating the discussion for the different phases of the model.

A. Quenches with $a < a_f$

In this section we present data for values of $a < a_f$. We have checked that for all the quenches studied in this sector one has $T_f \ll T_c(a)$, namely, that the target equilibrium state is in the ferromagnetic phase. According to the discussion of Sec. III A 1, when the quench is done in a phase where symmetry breaking occurs and $q_{\rm EA} > 0$, one expects an additive structure for the two-time quantities. For the autocorrelation, according to Eqs. (7) and (10), one should find data collapse, for any given value of $a < a_f$, by plotting $C(t, t_w) - C_{\rm eq}(t - t_w)$ against $L(t)/L(t_w)$. We have computed $C(t, t_w)$ in the quenched system and $C_{\rm eq}$ in the equilibrium state and the result of this plot is shown in Fig. 3 for different values of a. Notice that in this plot we use $L(t)/L(t_w) - 1$ on the x axis to better show the small time-difference regime. Figure 3 shows an excellent data collapse both for $a = 0.1$ and for $a = 0.3$ (a similar quality of the collapse is obtained also for other values of $a < a_f$, not shown here). This proves quite convincingly that the scaling structure described in Sec. III A 1 applies also to the present disordered case.

Notice that, for any $a > 0$, the scaling function g appearing in Eq. (10) is markedly different from the one of the pure case (plotted with a bold green curve). It must be kept in mind that this difference is trivially due, at least in part, to

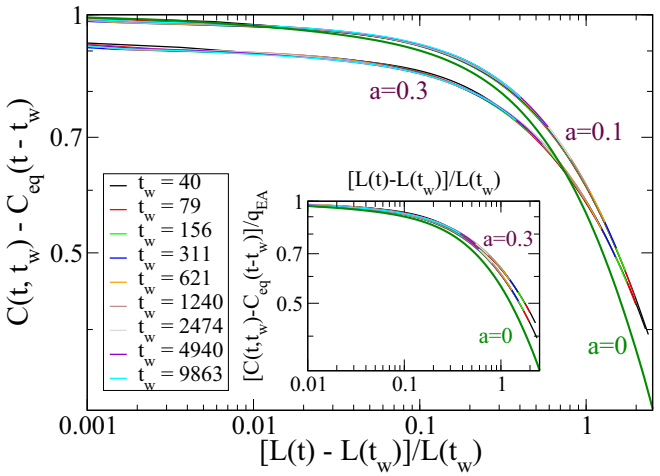

FIG. 3. $C(t, t_w) - C_{\rm eq}(t - t_w)$ is plotted against $L(t)/L(t_w) - 1$ for $a = 0.1$ (rightmost set of curves, see key), and $a = 0.3$ (lower set of curves, see key). For any value of a curves for different values of t_w are drawn with different colors, see key (these are difficult to distinguish because of an almost perfect data collapse). The heavy green curve is the scaling function $c(x)$ of the pure case with $a = 0$. In the inset we plot, for the same data, the quantity $[C(t, t_w) - C_{\rm eq}(t - t_w)]/q_{\rm EA}$.

the different value of $q_{\rm EA}$ as a changes. However, this fact is not sufficient to explain the differences between the curves for different a. To check this, we plot in the inset of Fig. 3 the quantity $[C(t, t_w) - C_{\rm eq}(t - t_w)]/q_{\rm EA}$ to eliminate the trivial difference of $q_{\rm EA}$ among the different cases. Here $q_{\rm EA} = m^2$ and the equilibrium squared magnetization m^2 has been measured numerically on the equilibrium states. The inset shows that the scaling function depends in a non trivial way on a and this is a clear indication that the *superuniversality* hypothesis [8,9], according to which scaling functions are universal and independent on the presence and strength of the quenched disorder, is not obeyed in the present system.

Let us now move to the analysis of the response function. The additive scheme implies that, for the response function, we should find data collapse by plotting $L(t_w)^{\alpha}[\chi(t, t_w) - \chi_{\rm eq}(t - t_w)]$ against $L(t)/L(t_w)$ [see Eq. (12)], where, in the absence of any reference theory, the response function exponent $\alpha > 0$ is considered as a fitting parameter. This kind of plot is presented in Fig. 4. Here we see that a good collapse of the data can be achieved in the region of large time separation (for large values of the abscissa) using values of $\alpha = 0.625, 0.2$ for $a = 0.1, 0.3$, respectively (values of α for different choices of a are plotted in the inset). The value of this exponent equals the one of the low-temperature pure case $\alpha = 0.625$ for $a = 0.1$, decreases markedly upon raising a and seems to vanish as $a \to a_f^-$, as it is shown in the inset of Fig. 4(b).

Notice that the data collapse presented in Fig. 4 is worst for smaller values of $L(t)/L(t_w)$, but improves as t_w grows larger and is always good for the larger values of this quantity. A similar pattern is observed also in ferromagnetic systems without disorder [10–23]. Let us also stress the fact that the scaling functions depend quite strongly on a, a fact that invalidates superuniversality, as already noticed studying the autocorrelation function.

B. Quenches with $a = a_f$

When the quench is made in a system with $a = a_f$ two main differences occur with respect to the previous case. The first is the fact that the finite T_f of our simulations corresponds to a quench into a disordered phase, since the critical temperature $T_c(a)$ of the ferromagnetic phase goes to zero as $a \to a_f^-$. This fact would suggest that the very asymptotic stage of the dynamics approaches the equilibrium state rapidly. However, due to the proximity of the critical point located at zero temperature, one expects to see slow evolution and aging in a transient preasymptotic stage. This is indeed observed in Fig. 2, where one sees that $L(t)$ keeps growing in a nearly power-law fashion at any time and there is no sign of convergence to an equilibrium value.

The second difference concerns the scaling properties of the two-time quantities. Indeed, at variance with the quenches with $a < a_f$, a quench made at $T_f = 0$ with $a = a_f$ is a quench at a critical point and hence one expects a multiplicative scaling structure as the one discussed in Sec. III A 2. This is further suggested by the fact that the equilibrium magnetization vanishes at a_f and hence $q_{\rm EA} = 0$ in this case. This same structure should characterize the two-time quantities

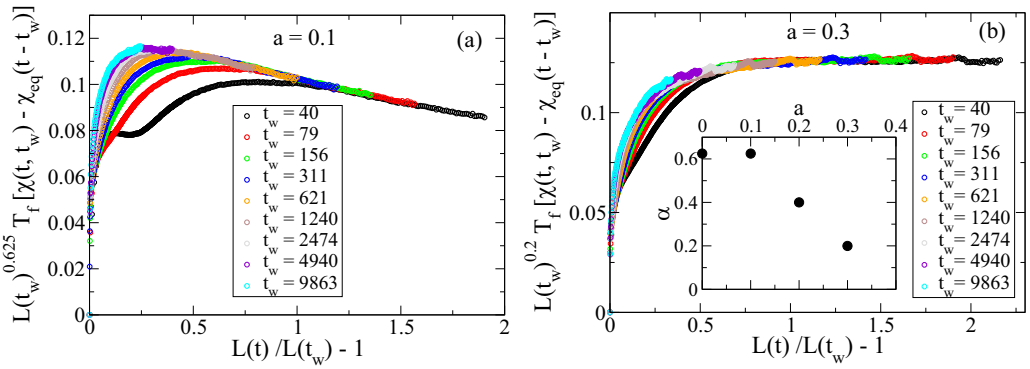

FIG. 4. $L(t_w)^{\alpha} T_f[\chi(t, t_w) - \chi_{\rm eq}(t - t_w)]$ is plotted against $L(t)/L(t_w) - 1$ for $a = 0.1$ [left panel (a)], and $a = 0.3$ [right panel (b)]. Curves for different values of t_w are drawn with different colors, see key. The values of α, which are reported in the inset of the right panel, are $\alpha = 0.625$ for $a = 0.1$, $\alpha = 0.4$ for $a = 0.2$, and $\alpha = 0.2$ for $a = 0.3$.

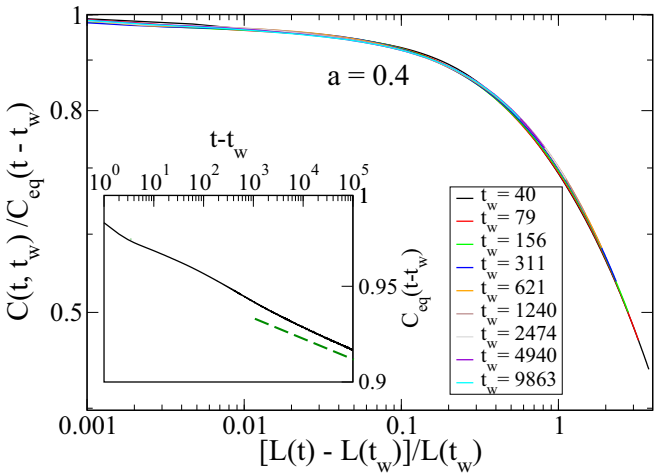

FIG. 5. $C(t, t_w)/C_{\rm eq}(t - t_w)$ is plotted against $L(t)/L(t_w) - 1$ for $a = 0.4$. Curves for different values of t_w are drawn with different colors; see key. In the inset the equilibrium correlation $C_{\rm eq}(t - t_w)$ is plotted against $t - t_w$. The green dashed line is the algebraic form $x^{-0.005}$.

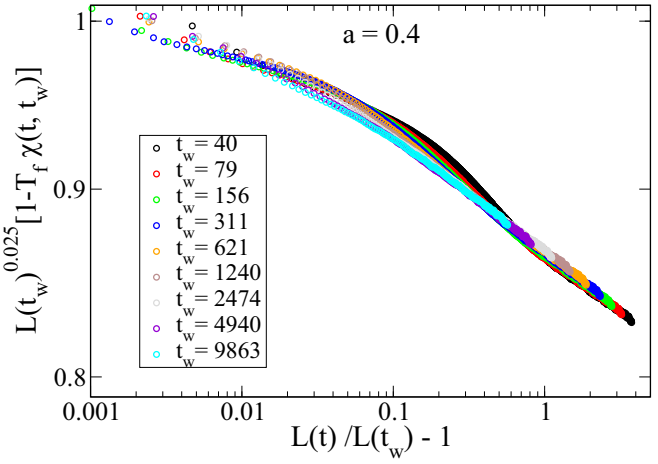

FIG. 6. $L(t_w)^{0.025}[1 - T_f\chi(t, t_w)]$ is plotted against $L(t)/L(t_w) - 1$ for $a = 0.4$. Curves for different values of t_w are drawn with different colors (see key).

also for quenches to finite temperatures, as the one we are studying numerically, provided they are sufficiently low to have a long-lasting aging stage. This is the case we consider here since for a quench right at $T_f = 0$ the system gets trapped in metastable states.

In Fig. 5 we plot the quantity $C(t, t_w)/C_{\rm eq}(t - t_w)$ against $L(t)/L(t_w)$, which, according to Eqs. (15) and (17) should amount to $C_{\rm ag}$ and provide data collapse of the curves with different t_w. Indeed, this is what one observes with great precision. This confirms that the multiplicative structure of a critical point is present. Let us add that the additive structure is definitely ruled out in this case also by the fact that $C_{\rm eq}(t, t_w) > C(t, t_w)$ for any $t > t_w$, so that, if an additive scheme would apply, one should have $C_{ag} = C - C_{\rm eq} < 0$, which is unphysical.

For completeness, let us briefly discuss the behavior of $C_{\rm eq}$, which is plotted in the inset of Fig. 5. It decays approximately as in Eq. (19) with a very small exponent $B \simeq 0.005$. From the data of Fig. 2 we see that, for sufficiently long times, $L(t)$ grows approximately in an algebraic way $L(t) \sim t^{1/z}$, with $z \simeq 5$ (this is the dashed indigo line in the figure). Hence, for the exponent γ defined in Eq. (21), we find $\gamma \simeq 0.025$, a fact that we will use soon.

We turn now to the discussion of the response function. According to the multiplicative scheme, one should find data collapse by plotting $L(t_w)^{\gamma}[1 - T_f\chi(t, t_w)]$ against $L(t)/L(t_w)$, as expressed by Eq. (21). The value of $\gamma \simeq 0.025$ has been estimated above from the properties of the autocorrelation function. We see in Fig. 6 that this value produces a good collapse of our data. Some residual oscillations, which are present particularly in the curve with smaller t_w, spoil somewhat the superposition, but these oscillation tend to decrease as t_w is taken larger and the collapse for the corresponding curves improves progressively.

It should be noted that the structure found in this quench cannot be framed among the scaling paradigms discussed in Sec. III for clean ferromagnetic systems, as we explain below. Since $T_c = 0$ for $a = a_f$, with this value of a the model can be interpreted as being at d_L. As discussed in Sec. III, in clean systems this would imply $\alpha = 0$. We see in the inset of Fig. 4, indeed, that the behavior of α as a is varied is consistent with the vanishing of this exponent as $a \to a_f$. In a clean system at $d = d_L$, however, one has a finite value of $q_{\rm EA}$, since the model is fully ordered at $T = 0$, which implies as additive scheme. In this case, instead, the point $(a = a_f, T = 0)$ is associated to a vanishing ferromagnetic order parameter, since it is the frontier with the paramagnetic region. Similarly, it is plausible that the spin-glass order parameter, which is finite at $T = 0$ for $a > a_f$, also vanishes as $a \to a_f^+$. From this point of view, then, the multiplicative structure that we find could be legitimate, since any order parameter vanishes in this critical point.

As a final remark, let us also mention that in clean magnetic systems with a scalar order parameter at $d = d_L$, as the Ising model in $d = 1$, the equilibrium parts of both C and χ vanish identically. This is not true in the present model at $a = a_f$, as we have shown. In a sense, the situation is reminiscent of what one has in a clean system with a vectorial order parameter, since in that case the response function is finite even at $T = 0$ due to the existence of the Goldstone modes. Possibly, the presence of soft modes is the origin of finite $C_{\rm eq}$ and $\chi_{\rm eq}$ also in the present model. These soft modes could arise as due to the peculiar character of interfaces, whose rearrangements might be enhanced by frustration as compared to what occurs in the ferromagnetic region.

C. Quenches with $a > a_f$

Even if the state of the system is disordered for any finite temperature when $a > a_f$ the steady growth of $L(t)$ observed in Fig. 2 signals that, in the range of times accessed in the simulations, the system is far from equilibration and the kinetics is slowed down due to the proximity of a critical region. Indeed, we know that not only a critical point exists at $(a = a_f, T = 0)$, but also the whole region $(a_f < a < a_a, T = 0)$ is presumably interested by a spin-glass phase [30]. For this reason we expect to detect scaling properties for

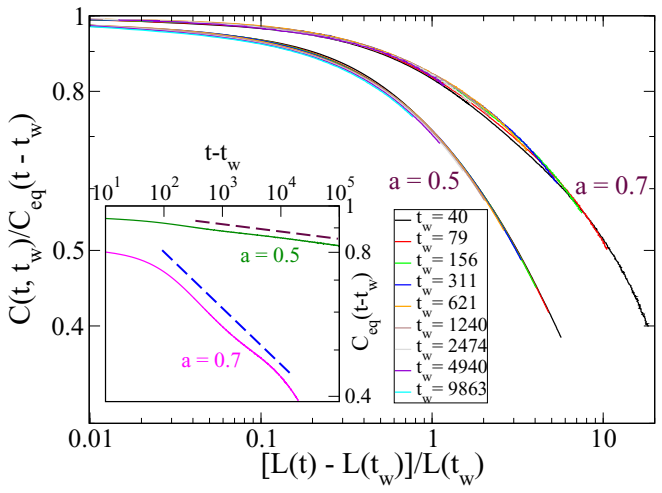

FIG. 7. $C(t, t_w)/C_{\rm eq}(t - t_w)]$ is plotted against $L(t)/L(t_w) - 1$ for $a = 0.5$ (lower set of curves) and $a = 0.7$ (upper set of curves). Curves for different values of t_w are drawn with different colors, see key. In the inset the quantity $C_{\rm eq}(t - t_w)$ is plotted for $a = 0.5$ and $a = 0.7$. The dashed maroon line is the behavior $x^{-0.0162}$ and the dashed blue is $x^{-0.12}$.

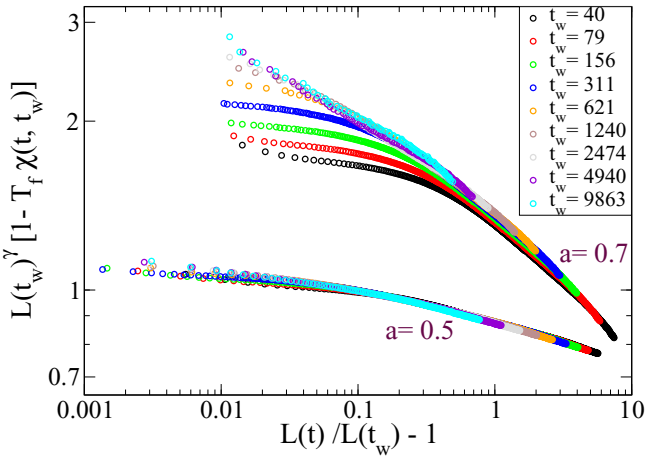

FIG. 8. $L(t_w)^{\gamma}[1 - T_f \chi(t, t_w)]$ is plotted against $L(t)/L(t_w) - 1$ for $a = 0.5$ (lower set of curves) and $a = 0.7$ (upper set of curves). Curves for different values of t_w are drawn with different colors, see key. The value of γ is $\gamma = 0.07$ for $a = 0.5$ and $\gamma = 0.3$ for $a = 0.7$

the two-time quantities. However, for this type of quenches, it is not obvious which scaling structure could emerge. Indeed, the system could feel the critical point at $(a = a_f, T = 0)$, in which case one would expect basically the same multiplicative structure observed in the quench at $a = a_f$ and with the same exponents. However, it is also possible that the influence of the spin-glass phase determines the behavior of the system. In this case, since in the spin-glass phase one has $q_{\rm EA}$, one could expect an additive structure to be appropriate.

Let us discuss the numerical data. First, as for the quench with $a > a_f$, we find that $C_{\rm eq}(t - t_w) > C(t, t_w)$ for any $t > t_w$, a fact that rules out the additive scheme. We show in Fig. 7 that, indeed, the multiplicative structure is very well verified. We mention that a similar multiplicative form for the autocorrelation was also found in the $3d$ spin-glass phase [48,54], although the matter is debated since different interpretations [49] may support either an additive structure. In our case, instead, this is definitely ruled out. Notice that also in this case the two curves depend on the amount of disorder a.

The equilibrium part $C_{\rm eq}$ of the autocorrelation (inset of Fig. 7) has a power-law decay as in Eq. (19), with an exponent $B \simeq 0.0162$. We stress that a power-law behavior of $C_{\rm eq}$ is usually found in spin-glass phases (for $d \geqslant 3$) [48,54]. Finally, let us remark that the oscillations of $C_{\rm eq}$ in the case $a = 0.7$ does not allow a clear statement about the behavior of this function.

Let us now discuss the behavior of the response function. In Fig. 8 we plot the quantity $L(t_w)^{\gamma}[1 - T_f \chi(t, t_w)]$ against $L(t)/L(t_w) - 1$ which, recalling the discussion above and Eq. (21), should result in a data collapse using $\gamma = Bz$. For $a = 0.5$, from the data of Fig. 2 we see that for sufficiently long times $L(t)$ grows approximately in an algebraic way $L(t) \sim t^{1/z}$, with $z \simeq 4.07$ (this is the brown dashed line) and hence $\gamma \simeq 0.066$. We can see in Fig. 8 that a good data collapse for the response function is obtained for a somewhat larger value $\gamma \simeq 0.07$. Given the noisy character of the problem and the possible presence of preasymptotic corrections we consider this value compatible with the general scaling framework.

For $a = 0.7$ we get a good superposition of the curves with different t_w with $\gamma = 0.3$. Notice that, both for $a = 0.5$ and $a = 0.7$, the collapse starts to be good earlier for large time differences [large $L(t)/L(t_w)$] and is worse for smaller time. This feature, however, is much more enhanced for $a = 0.7$. Nevertheless, also for $a = 0.7$ the superposition is satisfactory for the curves with larger t_w basically in the whole range of $L(t)/L(t_w)$. Using the growth exponent value $z \simeq 2.56$ obtained from the curve of $L(t)$ with $a = 0.7$ in Fig. 2, together with $\gamma = 0.3$, we get $B = \gamma/z \simeq 0.12$. In the inset of Fig. 7 we see that, indeed, this value of B is consistent with the decay of $C_{\rm eq}$, despite the presence of oscillations does not allow us to reach a definite conclusion.

Fluctuation-dissipation plot

In equilibrium the response function can be written in terms of the autocorrelation function using the fluctuation-dissipation theorem. Indeed, since both $\chi_{\rm eq}$ and $C_{\rm eq}$ depend only on $t - t_w$ a parametric form $\chi_{\rm eq}(t - t_w) = \widetilde{\chi}(C)$, with $T\widetilde{\chi}(C) = 1 - C$ (we stick here to spin systems) of the response in term of the autocorrelation can be arrived at. Out of equilibrium, when a nontrivial dependence on both the two times occurs, such a parametrization is not, in principle, possible. However, since C is usually a monotonic function, one can eliminate one of the two times, say t, from $\chi(t, t_w)$ in favor of C, thus obtaining $\chi(t, t_w) = \widehat{\chi}(C, t_w)$, and look at the parametric representation (or fluctuation-dissipation plot),

$$\widetilde{\chi}(C) = \lim_{t_w \to \infty} \widehat{\chi}(C, t_w), \tag{24}$$

if this limit exists. This relation is of great interest since it represents a bridge between the nonequilibrium dynamic properties, embodied by χ and C, and the static equilibrium

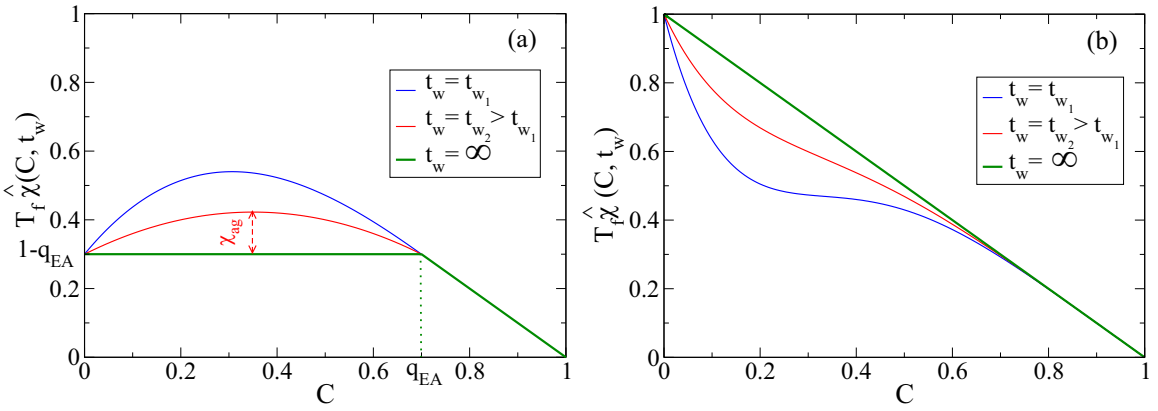

FIG. 9. Schematic representation of the approach of the curve $T_f\widehat{\chi}(C, t_w)$ to the asymptotic form $T_f\widetilde{\chi}(C)$ for a system with an additive scaling [left panel (a), see Sec. III A 1], and a multiplicative scaling [right panel (b), see Sec. III A 2]. Curves for different values of t_w are drawn with different colors; see key. The bold green curve with $t_w = \infty$ represents $T_f\widetilde{\chi}(C)$.

ones, represented by the overlap probability distribution $P(q)$ [1].

With the scaling forms of the two-time quantities discussed in Sec. III, for the additive (with $d > d_L$) and multiplicative cases in nondisordered systems one finds [33,55] the behavior that is schematically shown in Fig. 9. In this figure we not only plot the limiting form $\widetilde{\chi}(C)$ but also the approach of $\widehat{\chi}(C, t_w)$ to $\widetilde{\chi}(C)$ as t_w is progressively increased.

With the additive form one has the broken line,

$$T_f\widetilde{\chi}(C) = \begin{cases} 1 - q_{\rm EA}, & \text{for } C < q_{\rm EA} \\ 1 - C, & \text{for } C \geqslant q_{\rm EA}. \end{cases} \tag{25}$$

In this case the approach of $\widehat{\chi}(C, t_w)$ to $\widetilde{\chi}(C)$ as t_w increases is quite rapid for $C > q_{\rm EA}$, while it is much slower and occurs from above in the region $C < q_{\rm EA}$. It can be easily realized that the overshoot of $\widehat{\chi}$ with respect to $\widetilde{\chi}$ in this region is due to the nonequilibrium contribution $\chi_{\rm ag}$ whose asymptotic vanishing is regulated by the exponent α; see Eq. (12).

With the multiplicative structure, instead, the asymptotic form is the line $T_f\widetilde{\chi}(C) = 1 - C$, as in equilibrium. The approach of $\widehat{\chi}(C, t_w)$ to $\widetilde{\chi}(C)$ as t_w is increased is from below and convergence starts from larger values of C [Fig. 9(b)] and then progressively takes place at lower and lower values of C.

Let us now see how our numerical data behave. Examples of parametric plots for $a < a_f$ are shown in Fig. 10. In this figure the asymptotic form Eq. (25) has been drawn by taking $q_{\rm EA} = m^2$ and computing the equilibrium squared magnetization m^2 numerically on the equilibrium states. Notice that $1 - q_{\rm EA} \simeq 0$ for $a = 0.1$ since the equilibrium magnetization is $m \simeq 1$.

Regarding the approach of $\widehat{\chi}(C, t_w)$ to $\widetilde{\chi}(C)$, one observes a pattern qualitatively similar to the one shown in Fig. 9(a). Of course, the convergence is slow due to the limited range of t_w. Furthermore, since the overshoot of $\widehat{\chi}$ with respect to $\widetilde{\chi}$ is due to χ_{ag}, it disappears slower the smaller α is; see Eq. (12) and discussion above. Since α gets smaller upon raising a, this determines a slower convergence of the curves with $a = 0.3$

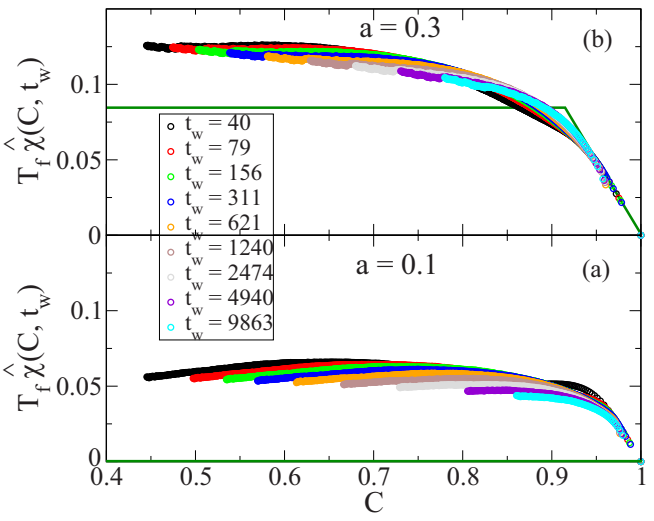

FIG. 10. $T_f\widehat{\chi}(C, t_w)$ is plotted against C for $a = 0.1$ [lower panel (a)] and $a = 0.3$ [upper panel (b)]. Curves for different values of t_w are drawn with different colors, see key. The bold green lines are the asymptotic forms $T_f\widetilde{\chi}(C)$.

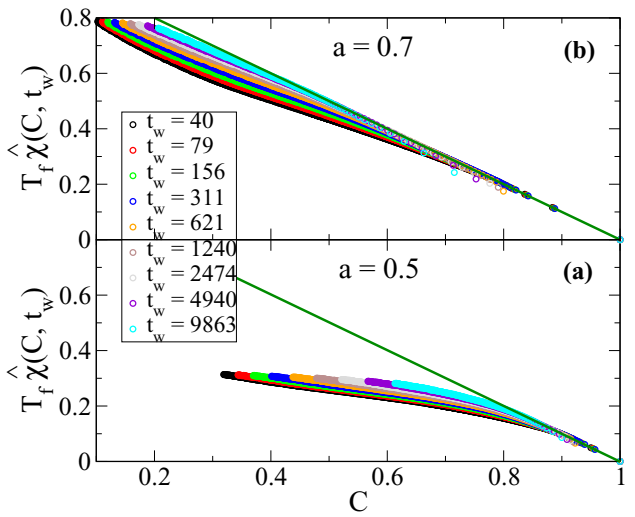

FIG. 11. $T_f\widehat{\chi}(C, t_w)$ is plotted against C for $a = 0.5$ [lower panel (a)] and $a = 0.7$ [upper panel (b)]. Curves for different values of t_w are drawn with different colors, see key. The bold green lines are the asymptotic form $T_f\widetilde{\chi}(C)$.

as compared to those with $a = 0.1$. Besides that, also the speed of growth of $L(t)$, which is a bit larger for $a = 0.1$ than for $a = 0.3$, plays a role in fostering the convergence of the curves. Notice also the anomalous feature (with respect to clean systems) of a slow convergence (from below) of the curves also for $C > q_{\rm EA}$, a fact that is possibly due to the slow character of the equilibrium states themselves.

According to our previous results, a multiplicative scheme applies in the whole region with $a \geqslant a_f$. Hence, in this region we expect to see a parametric plot qualitatively similar to the Fig. 9(b). Data from the simulations are presented in Fig. 11, confirming the expected behavior. In particular, for $a = 0.5$ the convergence toward $T_f \widetilde{\chi}(C) = 1 - C$ is rather slow, due to the very small value of the exponent γ ($\gamma \simeq 0.07$) and also to the slow growth of $L(t)$. For $a = 0.7$, γ takes the larger value $\gamma \simeq 0.3$ and $L(t)$ grows much faster, and this fact greatly speeds up the convergence of the curves. Indeed, we see that at the largest values of t_w the curve $\widetilde{\chi}(C)$ is almost attained.

V. CONCLUSIONS

The aim of this paper was to study how the scaling properties of two-time quantities, specifically the autocorrelation function and the associated response function, are affected by the presence of disorder and frustration in the kinetics of a magnetic system after a quench to a low temperature. To do that, we have studied numerically the model discussed in Ref. [30], which amounts to an Ising system in two dimensions where a fraction a of couplings take a negative value, while the remaining ones are ferromagnetic. Varying a this model interpolates between a clean ferromagnet at $a = 0$, a disordered ferromagnet for $0 < a < a_f$, and a paramagnet with a zero-temperature spin-glass phase for $a > a_f$.

Being two-dimensional, the model has the advantage of a relatively fast determination of the equilibrium states at low temperature in rather large systems, a fact that allows one to compute the equilibrium behavior of the two-time quantities with good accuracy. This has been utilized to address the issue of how equilibrium and aging degrees of freedom contribute to the kinetic evolution and how they combine to form the two-time quantities.

Our results show that this occurs quite differently in the different phases of the model. In particular, in the whole ferromagnetic region, for $0 \leqslant a \leqslant a_f$, one observes the same additive structure $C = C_{\rm eq} + C_{\rm ag}$ (and similarly for the response function) where the equilibrium and the aging parts sum up to form the complete correlation and response. This was expected and is consistent with the existence of a finite order parameter. Though the additive property applies to the entire ferromagnetic phase, the actual behavior of the two-time quantities turns out to be strongly dependent on the amount a of disorder. The response function exponent α, in particular, and the scaling functions, depend on a. This shows quite clearly that the property of superuniversality is not obeyed.

The fact that the response function exponent α vanishes in the limit $a \to a_f^-$ is of interest. Indeed this is what happens in clean magnets at the lower critical dimensionality and, in that context, it is interpreted as due to the fact that interfaces are free to move without experiencing any restoring force. For instance, Ising interfaces in $d = 1$ are pointlike random walkers. In the present case, one can provide a similar interpretation. Indeed, the model is at the lower critical dimension when $a = a_f$, since the critical temperature for ferromagnetism vanishes; see Fig. 1. Furthermore, it is conceivable that, due to the large amount of negative bonds along interfaces when $a = a_f$, these become soft objects whose displacement can occur rather freely as opposed to a clean (or weakly disordered) two-dimensional magnets where motion is driven by surface tension and curvature.

The additive structure breaks down at the critical point at $a = a_f$, and one sees a multiplicative one with $C = C_{\rm eq} C_{\rm ag}$. This might be considered consistent with what we know in clean magnets, since in that case a multiplicative structure emerges when the system is quenched to a critical point with a vanishing order parameter.

The same multiplicative structure is found when the system is quenched in the paramagnetic region with $a > a_f$. It must be observed that, although our quenches are done to finite temperatures and hence in the disordered phase of the model, in the range of times accessed in the simulations the system does not show any sign of equilibration. This can be ascribed to the zero-temperature spin-glass phase extending its influence to the preasymptotic evolution of the model. According to this interpretation, since in the spin-glass phase there is a nonvanishing order parameter, one should expect to find an additive structure for the two-time quantities. Instead, we have a clear indication of a multiplicative scheme, as already observed in other spin-glass systems [48,54], whose meaning remains to be clarified.

As a final remark, let us comment on the fact that the results of this paper, besides the interest in addressing general properties of the nonequilibrium kinetics of slowly relaxing systems, can help elucidating the structure of the phase-diagram of frustrated systems. In particular, the recognition of a different scaling paradigm, additive versus multiplicative, might enable one to distinguish between different phases, a fact that could turn out to be relevant and useful in the controversial field of frustrated systems. In this respect, the investigation of the properties of two-time quantities along the lines followed here in the three dimensional case represents an interesting research project for the future.

ACKNOWLEDGMENTS

Numerical results were obtained using the High-Performance Computing facility at IUAC, New Delhi (http://www.iuac.res.in/labs/hpcl/index.html). F.C. acknowledges financial support by MIUR Project No. PRIN2015K7KK8L.

[1] S. Franz, M. Mézard, G. Parisi, and L. Peliti, Phys. Rev. Lett. **81**, 1758 (1998); J. Stat. Phys. **97**, 459 (1999).

[2] F. Corberi, E. Lippiello, A. Mukherjee, S. Puri, and M. Zannetti, J. Stat. Mech.: Theory Exp. (2011) P03016.

[3] F. Corberi, E. Lippiello, A. Mukherjee, S. Puri, and M. Zannetti, Phys. Rev. E **85**, 021141 (2012).

[4] F. Corberi, E. Lippiello, A. Mukherjee, S. Puri, and M. Zannetti, Phys. Rev. E **88**, 042129 (2013).

[5] E. Lippiello, A. Mukherjee, S. Puri, and M. Zannetti, Europhys. Lett. **90**, 46006 (2010).

[6] C. Castellano, F. Corberi, U. Marini Bettolo Marconi, and A. Petri, J. Phys. IV France **08**, Pr6-93 (1998).

[7] F. Corberi, L. F. Cugliandolo, and H. Yoshino, Growing length scales in aging systems, in *Dynamical Heterogeneities in Glasses, Colloids, and Granular Media*, edited by L. Berthier, G. Biroli, J.-P. Bouchaud, L. Cipelletti, and W. van Saarloos (Oxford University Press, Oxford, 2011), pp. 370–406.

[8] L. F. Cugliandolo, Physica A **389**, 4360 (2010).

[9] D. S. Fisher and D. A. Huse, Phys. Rev. B **38**, 373 (1988).

[10] A. Barrat, Phys. Rev. E **57**, 3629 (1998).

[11] F. Corberi, E. Lippiello, and M. Zannetti, Phys. Rev. E **63**, 061506 (2001).

[12] F. Corberi, E. Lippiello, and M. Zannetti, Eur. Phys. J. B **24**, 359 (2001).

[13] M. Henkel, M. Pleimling, C. Godrèche, and J. M. Luck, Phys. Rev. Lett. **87**, 265701 (2001).

[14] M. Henkel and M. Pleimling, Phys. Rev. E **68**, 065101(R) (2003).

[15] M. Henkel, M. Paessens, and M. Pleimling, Europhys. Lett. **62**, 664 (2003).

[16] F. Corberi, E. Lippiello, and M. Zannetti, Phys. Rev. E **68**, 046131 (2003).

[17] F. Corberi, E. Lippiello, and M. Zannetti, Phys. Rev. Lett. **90**, 099601 (2003).

[18] F. Corberi, C. Castellano, E. Lippiello, and M. Zannetti, Phys. Rev. E **70**, 017103 (2004).

[19] F. Corberi, E. Lippiello, and M. Zannetti, Phys. Rev. E **72**, 056103 (2005).

[20] F. Corberi, E. Lippiello, and M. Zannetti, Phys. Rev. E **72**, 028103 (2005).

[21] E. Lippiello, F. Corberi, and M. Zannetti, Phys. Rev. E **71**, 036104 (2005).

[22] M. Henkel and M. Pleimling, Phys. Rev. E **72**, 028104 (2005).

[23] E. Lippiello, F. Corberi, and M. Zannetti, Phys. Rev. E **74**, 041113 (2006).

[24] E. Lippiello, F. Corberi, A. Sarracino, and M. Zannetti, Phys. Rev. E **78**, 041120 (2008).

[25] E. Lippiello, F. Corberi, A. Sarracino, and M. Zannetti, Phys. Rev. B **77**, 212201 (2008).

[26] M. Baiesi, C. Maes, and B. Wynants, Phys. Rev. Lett. **103**, 010602 (2009).

[27] F. Corberi, E. Lippiello, A. Sarracino, and M. Zannetti, Phys. Rev. E **81**, 011124 (2010).

[28] C. Godrèche and J. M. Luck, J. Phys.: Condens. Matter **14**, 1589 (2002).

[29] P. Calabrese and A. Gambassi, J. Phys. A: Math. Gen. **38**, R133 (2005).

[30] F. Corberi, M. Kumar, S. Puri, and E. Lippiello, Phys. Rev. E **95**, 062136 (2017).

[31] Y. Ozeki and H. Nishimori, J. Phys. Soc. Jpn. **56**, 1568 (1987).

[32] A. K. Hartmann, Phys. Rev. B **59**, 3617 (1999).

[33] F. Corberi, E. Lippiello and M. Zannetti, J. Stat. Mech. (2004) P12007.

[34] A. J. Bray, Adv. Phys. **43**, 357 (1994).

[35] P. C. Hohenberg and B. I. Halperin, Rev. Mod. Phys. **49**, 435 (1977).

[36] A. Coniglio, Physica A **281**, 129 (2000).

[37] F. Corberi, E. Lippiello, and M. Zannetti, Phys. Rev. E **74**, 041106 (2006)

[38] G. F. Mazenko, Phys. Rev. E **69**, 016114 (2004).

[39] G. F. Mazenko, O. T. Valls, and F. C. Zhang, Phys. Rev. B **31**, 4453 (1985).

[40] A. J. Bray, Phys. Rev. B **41**, 6724 (1990).

[41] E. Lippiello and M. Zannetti, Phys. Rev. E **61**, 3369 (2000).

[42] C. Godrèche and J. M. Luck, J. Phys. A: Math. Gen. **33**, 1151 (2000).

[43] F. Corberi, C. Castellano, E. Lippiello, and M. Zannetti, Phys. Rev. E **65**, 066114 (2002).

[44] F. Corberi, E. Lippiello, and M. Zannetti, Phys. Rev. E **65**, 046136 (2002).

[45] F. Corberi, A. de Candia, E. Lippiello, and M. Zannetti, Phys. Rev. E **65**, 046114 (2002).

[46] R. Burioni, D. Cassi, F. Corberi, and A. Vezzani, Phys. Rev. Lett. **96**, 235701 (2006).

[47] R. Burioni, D. Cassi, F. Corberi, and A. Vezzani, Phys. Rev. E **75**, 011113 (2007).

[48] L. Berthier and J.-P. Bouchaud, Phys. Rev. B **66**, 054404 (2002).

[49] L. D. C. Jaubert, C. Chamon, L. F. Cugliandolo, and M. Picco, J. Stat. Mech. (2007) P05001.

[50] L. F. Cugliandolo and J. Kurchan, Phys. Rev. Lett. **71**, 173 (1993); Philos. Mag. B **71**, 501 (1995).

[51] L. F. Cugliandolo and J. Kurchan, J. Phys. A **27**, 5749 (1994).

[52] M. Mezard, G. Parisi, and M. A. Virasoro, *Spin Glass Theory and Beyond* (World Scientific, Singapore, 1987).

[53] H. Khoshbakht and M. Weigel, Phys. Rev. B **97**, 064410 (2018).

[54] M. Manssen and A. K. Hartmann, Phys. Rev. B **91**, 174433 (2015).

[55] F. Corberi, E. Lippiello, and M. Zannetti, J. Stat. Mech. (2007) P07002.